Wake Steering Wind Farm Control With Preview Wind Direction Information

Preprint

Eric Simley, Paul Fleming, Jennifer King, and Michael Sinner

National Renewable Energy Laboratory

Presented at the 2021 American Control Conference
May 25–28, 2021

NREL is a national laboratory of the U.S. Department of Energy
Office of Energy Efficiency & Renewable Energy
Operated by the Alliance for Sustainable Energy, LLC

This report is available at no cost from the National Renewable Energy Laboratory (NREL) at www.nrel.gov/publications.

Contract No. DE-AC36-08GO28308

Conference Paper
NREL/CP-5000-79249
April 2021

Wake Steering Wind Farm Control With Preview Wind Direction Information

Preprint

Eric Simley, Paul Fleming, Jennifer King, and Michael Sinner

National Renewable Energy Laboratory

Presented at the 2021 American Control Conference
May 25–28, 2021

Suggested Citation
Simley, Eric, Paul Fleming, Jennifer King, Michael Sinner. 2021. *Wake Steering Wind Farm Control With Preview Wind Direction Information: Preprint*. Golden, CO: National Renewable Energy Laboratory. NREL/CP-5000-79249.
https://www.nrel.gov/docs/fy21osti/79249.pdf.

NREL is a national laboratory of the U.S. Department of Energy
Office of Energy Efficiency & Renewable Energy
Operated by the Alliance for Sustainable Energy, LLC

This report is available at no cost from the National Renewable Energy Laboratory (NREL) at www.nrel.gov/publications.

Contract No. DE-AC36-08GO28308

Conference Paper
NREL/CP-5000-79249
April 2021

National Renewable Energy Laboratory
15013 Denver West Parkway
Golden, CO 80401
303-275-3000 • www.nrel.gov

NOTICE

This work was authored by the National Renewable Energy Laboratory, operated by Alliance for Sustainable Energy, LLC, for the U.S. Department of Energy (DOE) under Contract No. DE-AC36-08GO28308. Funding provided by the U.S. Department of Energy Office of Energy Efficiency and Renewable Energy Wind Energy Technologies Office. The views expressed herein do not necessarily represent the views of the DOE or the U.S. Government. The U.S. Government retains and the publisher, by accepting the article for publication, acknowledges that the U.S. Government retains a nonexclusive, paid-up, irrevocable, worldwide license to publish or reproduce the published form of this work, or allow others to do so, for U.S. Government purposes.

This report is available at no cost from the National Renewable Energy Laboratory (NREL) at www.nrel.gov/publications.

U.S. Department of Energy (DOE) reports produced after 1991 and a growing number of pre-1991 documents are available free via www.OSTI.gov.

Cover Photos by Dennis Schroeder: (clockwise, left to right) NREL 51934, NREL 45897, NREL 42160, NREL 45891, NREL 48097, NREL 46526.

NREL prints on paper that contains recycled content.

Wake Steering Wind Farm Control With Preview Wind Direction Information

Eric Simley[1], Paul Fleming[1], Jennifer King[1], and Michael Sinner[1,2]

***Abstract*— Wake steering is a wind farm control strategy in which upstream turbines operate with a yaw misalignment to deflect their wakes away from downstream turbines, yielding a net power gain for the wind plant. But the inability of wake-steering controllers to perfectly track the wind direction leads to suboptimal performance. In this paper, we propose the use of preview wind direction measurements upstream of the turbine to improve controller performance by anticipating wind direction changes. Further, data from an operational wind plant are used to determine realistic preview measurement accuracy. Using the FLOw Redirection and Induction in Steady State (FLORIS) engineering wind farm control tool, we compare the performance of standard and preview-enabled baseline and wake-steering control for a two-turbine array during below-rated operation. Assuming perfect preview information, preview-based wake steering increases energy production by the equivalent of 8.9% of the baseline wake losses, compared to a wake loss recovery of 5.8% with standard wake steering. However, when realistic measurement accuracy is included, the preview-based controller provides no advantage over standard control, motivating the need for more sophisticated control and wind direction forecasting strategies.**

I. INTRODUCTION

Wake steering is a wind farm control strategy in which upstream turbines are misaligned with the wind direction, causing their wakes to deflect away from downstream wind turbines [1]. Although the misaligned wind turbines produce less power, the additional power generated by downstream turbines can yield a net power gain for the wind plant. Traditionally, the benefits of wake steering have been demonstrated assuming fixed wind directions (e.g., using high-fidelity modeling [2] or steady-state engineering wake models [3]). In practice, however, wake-steering controllers must operate in dynamic wind environments in which the wind conditions are estimated from imperfect measurements. A recent field demonstration of wake steering has shown a net increase in energy for specific wind directions [4], [5], but the inability of the controller to perfectly track the time-varying wind directions led to suboptimal performance. Specifically, the slow dynamics of the wind turbine's yaw controller, used to indirectly implement the desired yaw offsets, caused the offsets to lag behind the wind direction by up to several minutes [4].

Several strategies for addressing the challenges of wake steering in dynamic wind conditions have been investigated. Noticing that baseline yaw controllers react too slowly to yaw offset commands, Bossanyi [6] found that directly yawing wind turbines based on regularly updated yaw offsets increases wake-steering performance. With indirect yaw control, Kanev [7] observed that heavily filtering the wind directions used to determine the yaw offset, updating the offset command at least every 120 s, and including hysteresis on the yaw offsets yielded satisfactory energy gains and low levels of yaw activity. Several authors have investigated robust wake-steering control, in which yaw offsets are optimized assuming uncertainty in the wind directions the turbines experience (e.g., [8], [9]). Lastly, Doekemeijer *et al.* [10] and Howland *et al.* [11] proposed closed-loop wake-steering controllers that estimate plant-level wind conditions and wake model parameters in real time, demonstrating energy gains for six-turbine arrays using high-fidelity simulations.

Inspired by lidar-assisted wind turbine control, in which measurements of the approaching wind speeds are used to improve rotor speed regulation and reduce structural loads [12], we propose the use of preview wind direction information to improve wake steering. Preview measurements of the approaching wind directions are used as control inputs in place of measurements from the turbine's nacelle wind vane to help overcome controller delays [4], thus improving yaw tracking. To assess the impact of wind direction preview, we modify a wake-steering controller comprising a yaw offset lookup table combined with a standard yaw controller to accommodate wind direction measurements with varying amounts of preview. Preview measurements of the approaching wind direction could be obtained from several sources, including remote-sensing devices (e.g., lidar), meteorological masts, or one or more upstream wind turbines. For this study, we simply assume the wind direction is measured at a single point upstream of the turbine at hub height.

Preview wake steering is evaluated using the FLOw Redirection and Induction in Steady State (FLORIS) engi-

This work was authored by the National Renewable Energy Laboratory, operated by Alliance for Sustainable Energy, LLC, for the U.S. Department of Energy (DOE) under Contract No. DE-AC36-08GO28308. Funding provided by the U.S. Department of Energy Office of Energy Efficiency and Renewable Energy Wind Energy Technologies Office. The views expressed in the article do not necessarily represent the views of the DOE or the U.S. Government. The U.S. Government retains and the publisher, by accepting the article for publication, acknowledges that the U.S. Government retains a nonexclusive, paid-up, irrevocable, worldwide license to publish or reproduce the published form of this work, or allow others to do so, for U.S. Government purposes. Data were furnished to the authors under an agreement between the National Renewable Energy Laboratory, Siemens Gamesa Renewable Energy A/S, and Vattenfall. Data and results used herein do not reflect findings by Siemens Gamesa Renewable Energy A/S, and Vattenfall.

[1]National Wind Technology Center, National Renewable Energy Laboratory, Golden, CO 80401, USA. eric.simley@nrel.gov, paul.fleming@nrel.gov, jennifer.king@nrel.gov, michael.sinner@nrel.gov

[2]Department of Electrical, Computer, and Energy Engineering, University of Colorado, Boulder, CO 80309, USA. michael.sinner@colorado.edu

This report is available at no cost from the National Renewable Energy Laboratory (NREL) at www.nrel.gov/publications.

neering wind farm control tool [13] with stochastic wind direction inputs. Realistic preview measurement accuracy—limited by the evolving state of the atmosphere as the flow advects downstream—is included using a coherence model based on the measured correlation between wind directions along a row of wind turbines in a commercial wind plant. The coherence model is then used to introduce a preview distance-dependent correlation loss between the upstream measurements and the wind directions at the controlled turbine. For a two-turbine array, we evaluate the potential for preview wake steering, as well as preview baseline yaw control, assuming 1) perfect preview information, and 2) realistic preview measurement accuracy using the developed coherence model, but assuming no sensor error.

The remainder of the paper is organized as follows. In Section II, we describe the standard and preview-enabled wake-steering controllers evaluated here along with the baseline yaw controller used for comparison. The stochastic wind direction model is discussed in Section III. Section IV describes the FLORIS-based wake-steering simulation environment. Next, simulation results are provided in Section V. Finally, Section VI concludes the paper with recommendations for further research.

II. PREVIEW-BASED WAKE-STEERING CONTROLLER DESIGN

The wake-steering controller investigated here is based on a control architecture used in a recent field experiment [4], [5]. It comprises two stages: 1) a lookup-table-based wake-steering controller that outputs a yaw offset based on measured wind speed and direction, and 2) a baseline yaw controller that implements the desired yaw offset. In this section, we describe the baseline yaw controller as well as the standard and preview-enabled wake-steering controllers. To evaluate wake-steering control in this paper we consider a simple two-turbine array with a controlled turbine 5 rotor diameters ($5D$) due west of a waked turbine. The wind turbine parameters are based on the National Renewable Energy Laboratory (NREL) 5-MW reference wind turbine model [14] with D = 126 m and a rated wind speed of 11.4 m/s. Fig. 1a illustrates the upstream wind turbine operating with a +25° yaw misalignment, thereby redirecting its wake away from the downstream turbine.

A. Baseline yaw controller

The baseline yaw controller used by Simley *et al.* [9], based on the control strategy described by Bossanyi [6], is implemented here. The absolute wind direction measured by the turbine is filtered using a first-order filter with a time constant of 35 s (see Fig. 1b for definitions of wind direction ϕ, yaw position θ, and yaw offset/misalignment γ). When the magnitude of the difference between the low-pass-filtered wind direction and the turbine's yaw position exceeds a deadband threshold of 8°, the turbine begins yawing toward the wind direction at the rate of 0.3°/s assumed for the NREL 5-MW reference wind turbine [14]. Once the difference

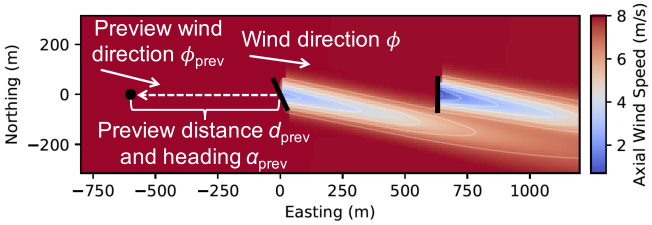

(a) Preview wake-steering scenario

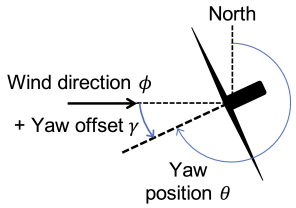

(b) Yaw control variables

Fig. 1: Wake-steering variables. (a) Wake steering scenario based on FLORIS showing preview distance and heading relative to north, wind direction, and preview wind direction. (b) Yaw position and yaw offset.

between the filtered wind direction and the yaw position reaches zero or changes sign, the turbine stops yawing.

B. Standard wake-steering controller

The standard wake-steering controller architecture investigated here was developed assuming yaw offsets must be applied indirectly using the wind turbine's existing yaw controller [4]. As shown in Fig. 2a, the wind direction (formed by summing the yaw position and the yaw misalignment measured by the wind vane) and the low-pass-filtered wind speed are used as inputs to a yaw offset lookup table. The selected yaw offset is then subtracted from the original wind vane signal. This modified vane signal is input to the yaw controller in place of the original vane measurement, thereby inducing the desired yaw offset. Note that Simley *et al.* [9] used a low-pass-filtered wind direction signal as the input to the lookup table; however, we found that energy production was maximized using the unfiltered wind direction for the wind conditions simulated here. In this work, we simplify the controller by assuming a constant wind speed of 8 m/s.

C. Robust yaw offsets

To determine the yaw offset schedule used in the lookup table shown in Fig. 2a, the optimal yaw offsets that maximize overall wind plant power are found using the FLORIS engineering wind farm control tool [13] for a sequence of wind directions in 1° steps. Following the reasoning explained by Fleming *et al.* [4], yaw offsets are constrained to be positive (a counterclockwise rotation of the nacelle relative to the wind direction [see Fig. 1b]). This constraint eliminates complexity associated with switching between large positive and negative offsets. Furthermore, positive yaw offsets have been shown to be more effective at redirecting wakes than negative yaw offsets [15], [16].

To address variability in the wind directions the controlled turbine will experience while operating at a given yaw

This report is available at no cost from the National Renewable Energy Laboratory (NREL) at www.nrel.gov/publications.

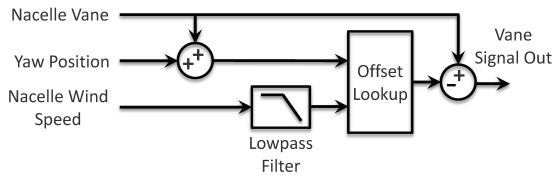

(a) Standard wake-steering controller

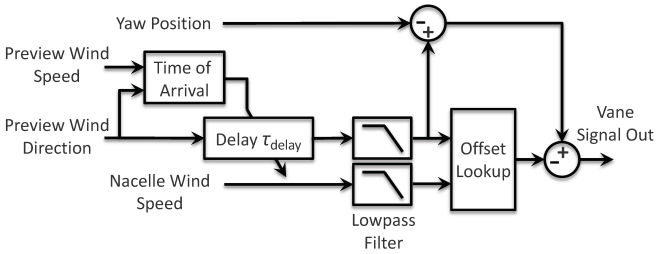

(b) Preview-based wake-steering controller

Fig. 2: Controller structure for (a) standard and (b) preview-based wake-steering controllers. The modified output vane signal is used as the input to the wind turbine's yaw controller.

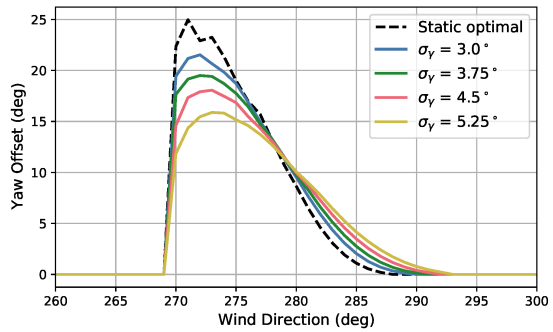

Fig. 3: Robust yaw offset schedules for a controlled wind turbine $5D$ west of a downstream turbine for a wind speed of 8 m/s. Optimal yaw offsets for different values of baseline yaw error standard deviation are compared to the static optimal offset schedule (without wind direction uncertainty). Wind turbine parameters are based on the NREL 5-MW reference turbine.

position, θ, we use robust yaw offset schedules. These are given by the yaw offsets that maximize the expected wind plant power production for a distribution of wind directions centered on the intended direction [8]–[9]. Based on the method presented by Simley *et al.* [9], a normal distribution of possible wind directions is used here. Assuming the yaw error contains contributions from wind direction variability as well as uncertainty in the yaw position achieved by the controller, the standard deviation of the wind direction variations, σ_ϕ, is given by

$$\sigma_\phi = \sqrt{\sigma_\gamma^2 - \sigma_\theta^2}, \tag{1}$$

where σ_γ is the yaw error standard deviation and σ_θ is the standard deviation of the yaw position uncertainty, approximated as 1.75° [9]. Examples of robust yaw offset schedules for a range of yaw error standard deviations are shown in Fig. 3.

D. Preview-based wake-steering controller

As shown in Fig. 2b, we made modifications to the standard wake-steering controller to allow preview wind direction measurements to be used in place of the turbine's nacelle wind vane. The upstream wind direction measurement is delayed by τ_{delay} s before it is filtered using a first-order low-pass filter and input to the yaw offset lookup table. Additionally, the wind vane signal used by the standard wake-steering controller is replaced by the difference between the filtered preview wind direction and the wind turbine's yaw position. Similar to lidar-assisted wind turbine control applications, the preview wind direction measurement is filtered to remove frequency components that are uncorrelated with the wind directions that arrive at the turbine [17]. The choice of filter time constant will be discussed in Section V.

The time delay, τ_{delay}, is intended to achieve a target preview time, τ_{prev}, and is given by

$$\tau_{\text{delay}} = \max\left(\tau_{\text{arrival}} - \tau_{\text{prev}}, 0\right), \tag{2}$$

where τ_{arrival} is the estimated time it takes for the measured wind to arrive at the turbine. Multiple values of τ_{prev}—which is used to overcome the delays caused by filtering as well as the slow dynamics of the baseline yaw controller—will be investigated when evaluating the controller in Section V. Using the preview distance, d_{prev}, and heading relative to north, α_{prev}, between the wind turbine and measurement locations (See Fig. 1a), τ_{arrival} is estimated as

$$\tau_{\text{arrival}} = d_{\text{prev}} / \left(\cos\left(\phi_{\text{prev,LPF}} - \alpha_{\text{prev}}\right) u_{\text{prev,LPF}}\right). \tag{3}$$

The variables $\phi_{\text{prev,LPF}}$ and $u_{\text{prev,LPF}}$ represent the upstream wind direction and wind speed measurements, respectively, each filtered using a first-order low-pass filter with a time constant of 60 s. This time constant is intended to approximate the slowly varying wind conditions governing the advection of the flow; identifying the optimal filter parameters requires further research.

III. WIND DIRECTION MODEL BASED ON FIELD MEASUREMENTS

We use data from an operational wind power plant to help simulate wake-steering control with realistic time-varying wind directions. Specifically, we analyze supervisory control and data acquisition data from the Lillgrund offshore wind plant, sampled at a resolution of 1 s, to determine 1) the power spectral density (PSD) of wind direction variations, and 2) the evolution of wind direction variations as the wind travels downstream. The Lillgrund wind plant—located between Denmark and Sweden—comprises 48 2.3-MW wind turbines, with a hub height of 65 m and D = 93 m, arranged in a regular grid with turbines spaced 400 m and 305 m apart in the two principle directions (see Fig. 4) [18].

Realistic wind direction evolution as the flow advects downstream is assessed by comparing the wind directions measured at three turbines separated by 400 m in the principle direction of 222°, as shown in Fig. 4. To reflect interest in wake steering during below-rated operation, the data are analyzed in 1-hour periods with mean wind speeds between 7 and 9 m/s. Furthermore, data are filtered to include only mean wind directions between 217° and 227°, when the flow is roughly aligned with the row of turbines. The resulting

This report is available at no cost from the National Renewable Energy Laboratory (NREL) at www.nrel.gov/publications.

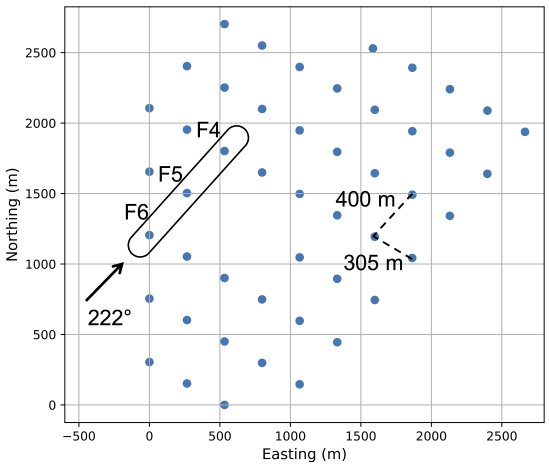

Fig. 4: Lillgrund wind farm layout showing the three turbines used to estimate the wind direction power spectral density and longitudinal coherence.

data set comprises 59 1-hour periods between May 2016 and March 2017. An example 1-hour period of measured wind directions is provided in Fig. 5a, where the propagation delay between the three turbine locations is shown.

Rather than directly using the observed wind direction time series for wake-steering simulations, a statistical wind direction model is used to generate realistic stochastic wind direction time series, as will be explained in Section IV. Therefore, an arbitrary number of simulations can be performed. The wind directions along the row of three turbines are characterized by the PSD of the free-stream wind direction variations at wind turbine F6 as well as the longitudinal coherence between the wind directions measured at F6 and both F5 and F4. The PSD of the wind direction, ϕ, at F6 is plotted in Fig. 5b along with a simple model fit given by

$$S_{\phi\phi}(f) = \frac{2.2 \cdot 10^3 \sigma_\phi^2}{\left(1 + \frac{f}{9 \cdot 10^{-4}}\right)^3}, \tag{4}$$

where σ_ϕ indicates the 1-hour wind direction standard deviation. Based on all 59 hours of data, $\sigma_\phi \approx 8°$. The upstream turbine F6 is used to estimate the wind direction PSD because the wind directions at F5 and F4 exhibit signs of high-frequency wake-added turbulence (see Fig. 5a).

The correlation between preview measurements of the wind direction, ϕ_{prev}, obtained at F6 and the actual wind directions, ϕ, that arrive at F5 and F4 is characterized using the longitudinal magnitude squared coherence function

$$\gamma^2_{\phi\phi_{\text{prev}},\text{long}}(f) = \frac{\left|S_{\phi\phi_{\text{prev}}}(f)\right|^2}{S_{\phi\phi}(f)\, S_{\phi_{\text{prev}}\phi_{\text{prev}}}(f)}, \tag{5}$$

describing the correlation (from 0 to 1) between the signals as a function of frequency. The function $S_{\phi\phi_{\text{prev}}}(f)$ is the cross-spectral power density between the upstream and downstream wind directions, whereas $S_{\phi\phi}(f)$ and $S_{\phi_{\text{prev}}\phi_{\text{prev}}}(f)$ are the PSDs of the downstream and preview wind directions, respectively. Note that ϕ_{prev} is time shifted by the estimated arrival time given by Eq. 3 before the coherence is calculated. Figure 5c contains the measured longitudinal coherence between the time-shifted wind directions at F6 and the wind directions that arrive at F5 and F4, 400 m and 800 m downstream, respectively. To model coherence for arbitrary preview distances, d_{prev}, an exponential decay coherence function is fit to the measured coherence curves in Fig. 5c, given by

$$\gamma^2_{\phi\phi_{\text{prev}},\text{long}}(f) = \exp\left(-\frac{7}{8} d_{\text{prev}} f\right). \tag{6}$$

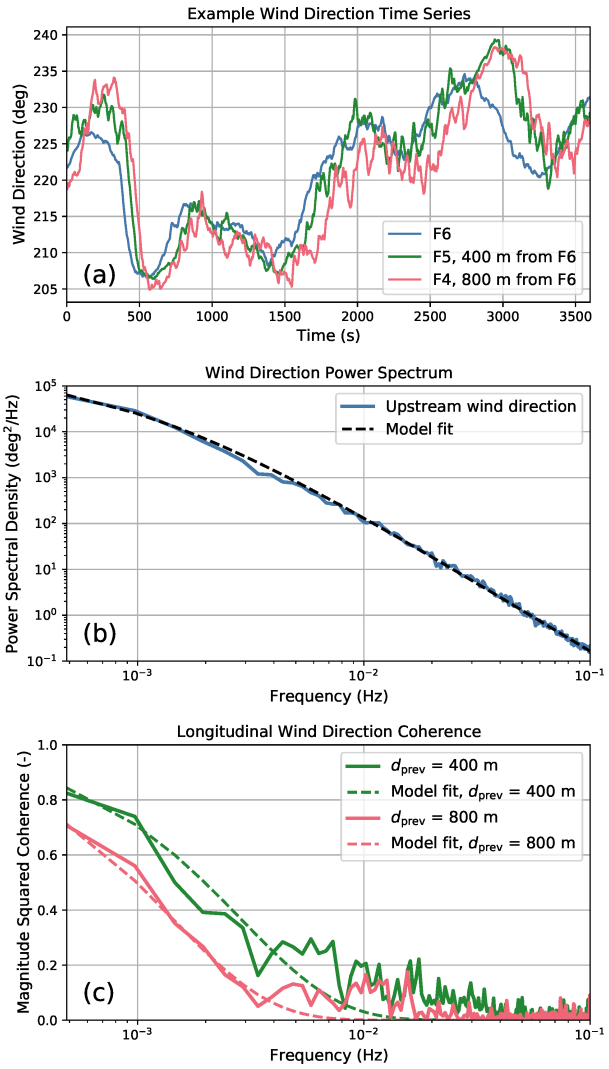

Fig. 5: Characterization of 1-hour wind directions at turbines F6, F5, and F4 for 1-hour mean wind speeds from 7-9 m/s and mean wind directions from 217-227°. (a) Example time series. (b) Power spectral density of wind direction at turbine F6 and model fit given by Eq. 4. (c) Longitudinal coherence between wind direction at turbine F6, time-shifted using Eq. 3, and wind directions at turbines F5 and F4, together with model fit (Eq. 6).

IV. SIMULATION ENVIRONMENT

In this section, we briefly describe the FLORIS model used to simulate wake steering, the stochastic wind direction inputs, and the overall simulation strategy.

This report is available at no cost from the National Renewable Energy Laboratory (NREL) at www.nrel.gov/publications.

A. FLORIS model

Wake steering is simulated using FLORIS for the array of two NREL 5-MW reference wind turbines separated by $5D$ in the east-west direction shown in Fig. 1a. We use the default Gauss-Curl Hybrid wake velocity and deflection model within FLORIS [19], with an ambient turbulence intensity value of 8%—found to closely match results from a wake-steering field experiment [5]—at a fixed below-rated mean wind speed of 8 m/s. The impact of yaw misalignment, γ, on power production is modeled by scaling the power by $(\cos\gamma)^{1.9}$, where the exponent of 1.9 was estimated by Gebraad *et al.* [2] based on high-fidelity modeling.

B. Stochastic wind directions

Following the Veers method for generating stochastic wind fields using frequency domain techniques [20], we treat the time-delayed preview wind direction measurement, ϕ_{prev}, and downstream wind direction, ϕ, as jointly Gaussian random processes. Using the coherence model in Eq. 6 to describe the correlation between the two wind directions and the PSD given by Eq. 4 to define their power spectra, multiple stochastic realizations of the wind direction time series can be generated for a given preview distance. Although the FLORIS model assumes a constant wind speed of 8 m/s, the error associated with estimating the arrival time, $\tau_{arrival}$, of the measured wind in real time is inherent in the longitudinal coherence model, as explained in Section III.

Although the standard yaw and wake-steering controllers act on the full wind direction measurements, ϕ, a low-pass-filtered version of the original wind direction signal, ϕ_ℓ, is used as the input to FLORIS. Because the steady-state FLORIS wake model inherently captures some of the high-frequency wind direction variations via ambient turbulence, the wind direction input should ideally reflect the slowly varying large-scale mean wind direction across the wind power plant. Although it is difficult to determine which frequencies should be attributed to ambient turbulence and which represent large-scale variations, we approximate the separation by filtering the original wind direction signal using a first-order filter with a cutoff frequency of 0.0011 Hz. This particular frequency is estimated by comparing the power spectra of wind directions from a stationary large-eddy simulation used to tune FLORIS and wind directions measured in the field, as discussed by Simley *et al.* [9].

C. Simulation overview

The impact of preview wind direction information is assessed for a range of preview distances. For each preview distance, two preview measurement scenarios are investigated: 1) an ideal scenario with perfect preview information, where the preview measurement is simply a time-shifted copy of the downstream wind direction signal, and 2) a realistic scenario relying on the longitudinal coherence model. Within both preview scenarios, four types of controllers are simulated: 1) standard baseline yaw control, 2) preview-enabled baseline yaw control, 3) standard wake-steering control, and 4) preview-enabled wake steering. Note that the realistic preview scenario is intended to capture measurement error caused by the evolution of the atmosphere as the flow advects downstream. In practice, additional error sources could exist (e.g., sensor error and complex terrain effects).

For each preview measurement scenario, 3240 stochastic 1-hour realizations of the wind direction time series are generated using a 1-s sample period, with mean wind directions evenly distributed between 230° and 310° (thereby encompassing the entire waked sector). For each time series, the baseline yaw controller is simulated with and without preview. The resulting yaw error standard deviations, σ_γ, are used to determine the robust yaw offset schedules for the wake-steering controllers. Next, standard and preview-based wake-steering control is simulated. For all simulations, the yaw position of the downstream turbine is determined using either standard or preview-enabled baseline yaw control. Results from the first 15 minutes of each 1-hour simulation are discarded to remove controller startup transients. Lastly, the resulting low-frequency wind direction and yaw position combinations are used to determine the expected energy production using FLORIS. Because FLORIS models time-averaged flow, we treat the downstream wind turbine's power at a particular time step as the expected power after the wake from the upstream turbine has propagated downstream.

Examples of the stochastic wind direction signals and simulated yaw positions for the upstream wind turbine with baseline and wake-steering control are provided in Fig. 6 for standard and preview-enabled control, with both ideal and realistic preview measurements.

V. PREVIEW-BASED WAKE-STEERING SIMULATION RESULTS

Simulation results for baseline and wake-steering control are presented here for standard and preview-based control strategies using preview distances, d_{prev}, from 80 to 1120 m, corresponding to preview times, τ_{prev}, from 10 to 140 s for the mean wind speed of 8 m/s. Results are provided for both ideal and realistic preview measurements. For the ideal preview scenario, we filter the preview wind direction measurement using a time constant of 30 s (see Fig. 2b), which maximizes energy production with wake steering. However, for the realistic preview scenario, we use unfiltered preview measurements; the time delay introduced by filtering leads to less effective yaw tracking and lower energy production.

A. Preview-based yaw control performance

First, the control improvement using preview wind direction information is assessed for baseline yaw control (equivalent to using the preview-based wake-steering controller in Fig. 2b without yaw offsets). Figure 7a compares the yaw error standard deviation, σ_γ, for standard yaw control as well as ideal and realistic preview control as a function of preview time and distance. The yaw error, γ, is defined with respect to the low-frequency wind direction, ϕ_ℓ, which is used as the input to FLORIS. As shown in Fig. 7a, ideal preview-based yaw control reduces the yaw error standard deviation relative to the baseline value of $\sigma_\gamma = 4.2°$, achieving a

This report is available at no cost from the National Renewable Energy Laboratory (NREL) at www.nrel.gov/publications.

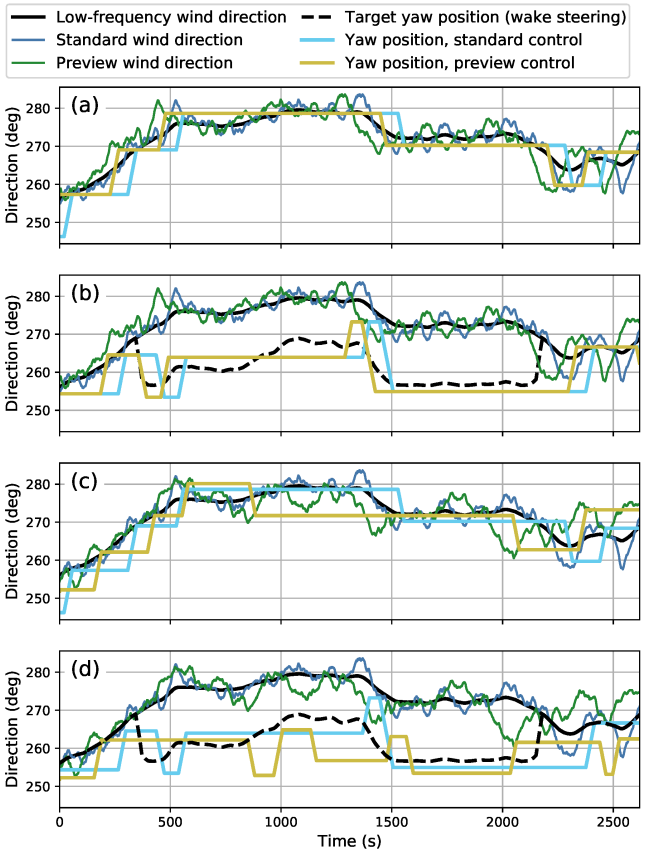

Fig. 6: Example simulation time series comparing standard and preview-based control for the upstream wind turbine for the (a) baseline and (b) wake-steering controllers with ideal preview measurements as well as the (c) baseline and (d) wake-steering controllers with realistic preview. The simulations use a preview time of τ_{prev} = 80 s (a preview distance of d_{prev} = 640 m for the mean wind speed of 8 m/s). Each plot shows the low-frequency wind direction, ϕ_ℓ, standard wind direction measurement, ϕ, preview wind direction measurement, ϕ_{prev}, as well as yaw positions, θ, with standard and preview control. For plots (b) and (d), the target yaw positions for wake steering are shown.

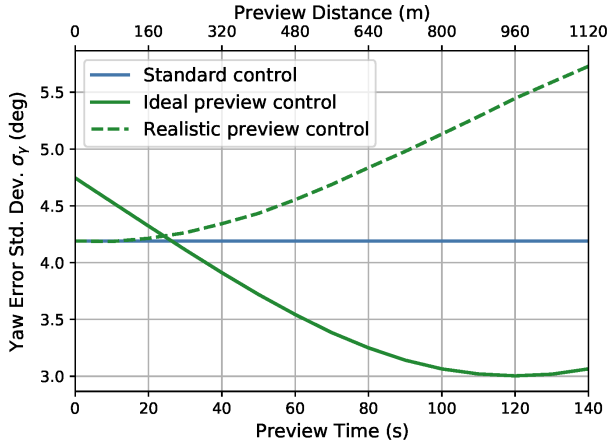

(a) Yaw error standard deviation with baseline yaw control

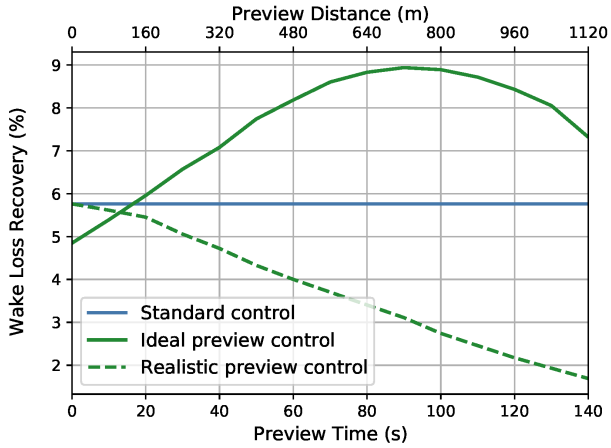

(b) Wake loss recovery from wake steering

Fig. 7: Control performance for standard control, ideal preview control, and realistic preview control for different preview times and distances. (a) Yaw error standard deviation for baseline yaw control. (b) Percentage of total wake losses recovered from wake steering.

minimum standard deviation of 3.0°, with 120 s of preview. With additional preview time, the controller tends to yaw too early, tracking the upcoming wind directions less effectively. Note that ideal preview-based control performs worse than standard yaw control for preview times less than 30 s because of the time delay introduced by the measurement filter. With realistic preview measurements, there appears to be no benefit to using preview information. The amount of yaw error continues to grow as the preview time increases.

Although not presented here, reducing yaw error through the use of preview information improves energy capture with baseline yaw control in addition to wake steering.

B. Preview-based wake steering performance

Wake-steering performance is expressed in terms of the percentage of wake losses incurred with baseline yaw control that are recovered by wake steering, similar to analysis by Fleming *et al.* [5]. Wake losses are determined by comparing the total energy production of the wind turbines to the total energy that would have been produced if both turbines were unwaked and operating with baseline yaw control. Therefore, the wake loss recovery from wake steering is calculated as

$$\Delta_{L_{\text{wake}}} = 1 - \frac{\sum_{i=1}^{N} \left(2P_{\text{up,base},i} - P_{\text{total,control},i}\right)}{\sum_{i=1}^{N} \left(2P_{\text{up,base},i} - P_{\text{total,base},i}\right)}, \qquad (7)$$

where $P_{\text{up,base},i}$ and $P_{\text{total,base},i}$ represent the power produced by the upstream turbine and the total power produced by the array, respectively, with baseline yaw control for the i-th 1-hour simulation. Similarly, $P_{\text{total,control},i}$ indicates the total power produced by the array with wake steering.

The wake loss recovery from wake steering is presented in Fig. 7b for standard as well as ideal and realistic preview-based wake steering as a function of preview time and distance. The energy gained by the standard wake-steering controller is equivalent to 5.8% of the baseline wake losses. With ideal measurements, the preview-based wake-steering controller recovers a maximum of 8.9% of the baseline wake losses with 90 s of preview, representing a 55% increase in energy *gain* compared to standard wake steering. As can be expected from the yaw errors in Fig. 7a, preview-based wake

This report is available at no cost from the National Renewable Energy Laboratory (NREL) at www.nrel.gov/publications.

steering with realistic preview measurements performs worse than standard wake steering. Further, the wake loss recovery decreases as the preview distance increases, indicating that the marginal benefit of extra preview time is outweighed by the lower measurement coherence.

VI. DISCUSSION AND CONCLUSIONS

In this paper, we modified a simple wake-steering controller to allow the use of preview wind direction information, with the goal of improving yaw tracking in dynamic wind conditions. Using data from an offshore wind power plant, we developed a method for generating realistic wind direction measurements to evaluate preview-based wake steering. We performed simulations for a two-turbine array using the FLORIS model to determine power production for different control scenarios. With perfect preview information, preview-based wake steering was found to increase energy production significantly more than standard wake steering, with a preview time of 90 s providing the most benefit.

We expect the optimal preview time to depend on the yaw controller dynamics and wind conditions. For controllers that yaw less frequently, longer preview times will likely be needed to overcome controller lag. But for more responsive controllers, or when operating in highly variable wind conditions, shorter preview times should help ensure the yaw position does not lead the wind direction too much.

With realistic preview measurement accuracy, on the other hand, no improvement in wake-steering performance was observed. However, the wind direction coherence model we used to determine preview measurement accuracy represents the average coherence for a variety of atmospheric conditions. More research is needed to determine how longitudinal wind direction coherence depends on atmospheric conditions as well as terrain. Particular sites or wind conditions may be more favorable for preview-based wake steering.

To fully evaluate the benefits of preview-enabled wake steering with realistic measurement accuracy, more sophisticated control strategies should be explored. For example, rather than waiting for the wind turbine's existing yaw controller to implement wake steering, additional performance gains could be made by yawing the turbine more frequently, (e.g., at fixed time intervals [6], [10]). Further, model predictive control approaches could be used to explicitly optimize the control actions based on the wind direction preview.

In addition to yaw controller improvements, more effective methods for estimating the approaching wind directions should be investigated. For instance, Annoni *et al.* [21] present a consensus approach for estimating local wind directions through information exchange between wind turbines that could improve forecasting accuracy. Moreover, remote-sensing devices, such as scanning lidars, could be used to measure the approaching wind conditions over a large area.

REFERENCES

[1] S. Boersma, B. M. Doekemeijer, P. M. O. Gebraad, P. A. Fleming, J. Annoni, A. K. Scholbrock, J. A. Frederik, and J. W. V. Wingerden, "A tutorial on control-oriented modeling and control of wind farms," in *American Control Conference*, Seattle, WA, 2017, pp. 1–18.

[2] P. Gebraad, F. Teeuwisse, J. Wingerden, P. A. Fleming, S. Ruben, J. Marden, and L. Pao, "Wind plant power optimization through yaw control using a parametric model for wake effects–a CFD simulation study," *Wind Energy*, vol. 19, no. 1, pp. 95–114, 2016.

[3] P. Gebraad, J. J. Thomas, A. Ning, P. Fleming, and K. Dykes, "Maximization of the annual energy production of wind power plants by optimization of layout and yaw-based wake control," *Wind Energy*, vol. 20, no. 1, pp. 97–107, 2017.

[4] P. Fleming, J. King, K. Dykes, E. Simley, J. Roadman, A. Scholbrock, P. Murphy, J. K. Lundquist, P. Moriarty, K. Fleming, J. van Dam, C. Bay, R. Mudafort, H. Lopez, J. Skopek, M. Scott, B. Ryan, C. Guernsey, and D. Brake, "Initial results from a field campaign of wake steering applied at a commercial wind farm – part 1," *Wind Energy Science*, vol. 4, no. 2, pp. 273–285, 2019.

[5] P. Fleming, J. King, E. Simley, J. Roadman, A. Scholbrock, P. Murphy, J. K. Lundquist, P. Moriarty, K. Fleming, J. van Dam, C. Bay, R. Mudafort, D. Jager, J. Skopek, M. Scott, B. Ryan, C. Guernsey, and D. Brake, "Continued results from a field campaign of wake steering applied at a commercial wind farm – part 2," *Wind Energy Science*, vol. 5, no. 3, pp. 945–958, 2020.

[6] E. Bossanyi, "Combining induction control and wake steering for wind farm energy and fatigue loads optimisation," *Journal of Physics: Conference Series*, vol. 1037, no. 3, p. 032011, 2018.

[7] S. Kanev, "Dynamic wake steering and its impact on wind farm power production and yaw actuator duty," *Renewable Energy*, vol. 146, pp. 9–15, 2020.

[8] A. Rott, B. Doekemeijer, J. K. Seifert, J.-W. van Wingerden, and M. Kühn, "Robust active wake control in consideration of wind direction variability and uncertainty," *Wind Energy Science*, vol. 3, no. 2, pp. 869–882, 2018.

[9] E. Simley, P. Fleming, and J. King, "Design and analysis of a wake steering controller with wind direction variability," *Wind Energy Science*, vol. 5, no. 2, pp. 451–468, 2020.

[10] B. M. Doekemeijer, D. van der Hoek, and J.-W. van Wingerden, "Closed-loop model-based wind farm control using floris under time-varying inflow conditions," *Renewable Energy*, vol. 156, pp. 719–730, 2020.

[11] M. F. Howland, A. S. Ghate, S. K. Lele, and J. O. Dabiri, "Optimal closed-loop wake steering – part 1: Conventionally neutral atmospheric boundary layer conditions," *Wind Energy Science*, vol. 5, no. 4, pp. 1315–1338, 2020.

[12] A. Scholbrock, P. Fleming, D. Schlipf, A. Wright, K. Johnson, and N. Wang, "Lidar-enhanced wind turbine control: Past, present, and future," in *American Control Conference*, Boston, MA, July 2016, pp. 1399–1406.

[13] NREL, "FLORIS. Version 2.2.4," 2020. [Online]. Available: https://github.com/NREL/floris

[14] J. M. Jonkman, S. Butterfield, W. Musial, and G. Scott, "Definition of a 5-MW reference wind turbine for offshore system development, NREL/TP-500-38060," National Renewable Energy Laboratory, Golden, CO, Tech. Rep., 2009.

[15] P. Fleming, J. Annoni, M. Churchfield, L. A. Martinez-Tossas, K. Gruchalla, M. Lawson, and P. Moriarty, "A simulation study demonstrating the importance of large-scale trailing vortices in wake steering," *Wind Energy Science*, vol. 3, no. 1, pp. 243–255, 2018.

[16] R. Nouri, A. Vasel-Be-Hagh, and C. L. Archer, "The Coriolis force and the direction of rotation of the blades significantly affect the wake of wind turbines," *Applied Energy*, vol. 277, p. 115511, 2020.

[17] E. Simley and L. Pao, "Reducing lidar wind speed measurement error with optimal filtering," in *American Control Conference*, Washington, D.C., 2013, pp. 621–627.

[18] S. Ivanell, K. Nilsson, O. Eriksson, S. Sderberg, and I. Carln, "Wind turbine wakes and wind farm wakes, report 2018:541," Energiforsk, Stockholm, Sweden, Tech. Rep., 2018.

[19] J. King, P. Fleming, R. King, L. A. Martínez-Tossas, C. J. Bay, R. Mudafort, and E. Simley, "Controls-oriented model for secondary effects of wake steering," *Wind Energy Science Discussions*, vol. 2020, pp. 1–22, 2020.

[20] P. Veers, "Three-dimensional wind simulation, SAND88-0152," Sandia National Laboratories, Albuquerque, NM, Tech. Rep., 1988.

[21] J. Annoni, C. Bay, K. Johnson, E. Dall'Anese, E. Quon, T. Kemper, and P. Fleming, "Wind direction estimation using scada data with consensus-based optimization," *Wind Energy Science*, vol. 4, no. 2, pp. 355–368, 2019.

This report is available at no cost from the National Renewable Energy Laboratory (NREL) at www.nrel.gov/publications.